

TRANSITION METAL COMPLEXES WITH UNINEGATIVE BIDENTATE SCHIFF BASE

Synthetic, thermal, spectroscopic and coordination aspects

C. K. Modi, S. H. Patel and M. N. Patel*

Department of Chemistry, Sardar Patel University, Vallabh Vidyanagar, Gujarat 388 120, India

The present article describes the synthesis, structural features and thermal studies of the complexes of the type $[M(SB)_2(H_2O)] \cdot nH_2O$ [where HSB=pyridine-*m*-carboxaldene-*o*-aminobenzoic acid and $M=Mn(II)$, $Co(II)$, $Ni(II)$, $Cu(II)$, $Zn(II)$ and $Cd(II)$]. The complexes have been characterized on the basis of elemental analyses, magnetic susceptibility measurements, (FTIR and electronic) spectra and thermal studies. The nature of the bonding has been discussed on the basis of infrared spectral data. Magnetic susceptibility measurements and electronic spectral data suggest a six-coordinated structure of these complexes. The complexes of $Mn(II)$, $Co(II)$, $Ni(II)$, $Cu(II)$ are paramagnetic, while $Zn(II)$ and $Cd(II)$ are diamagnetic in nature.

The thermal decomposition of the complexes have been studied and indicates that not only the crystallization and coordinated water are lost but also that the decomposition of the ligand from the complexes is necessary to interpret the successive mass losses. The kinetic parameters such as order of reaction (n) and the energy of activation (E_a) have been reported using Freeman–Carroll method. The entropy (S^*), the pre-exponential factor (A), the enthalpy (H^*) and the Gibbs free energy (G^*) have been calculated.

Keywords: divalent transition metal complexes, DSC studies, DTA studies, spectroscopic analyses, TG/DTG
uninegative bidentate Schiff base

Introduction

Schiff bases and their metal complexes played a key role in our understanding of the coordination chemistry of transition metal ions. The field of Schiff base complexes was fast developing on account of the wide variety of possible structures for the ligands depending upon the aldehydes and amines [1]. The combination of distinctly different metal ion binding sites within one ligand could lead to materials with interesting new properties [2, 3] e.g. specific sensors, molecular wires, magnetic and optical devices. The thermal analysis techniques were extensively applied in studying of the thermal behaviour of metal complexes [4–10]. Differential scanning calorimetry (DSC) and differential thermal analysis (DTA) procedures permit the determination of non-isothermal transformation kinetics [11]. In continuation of our earlier work [12, 13] herein we describe synthetic, spectral, thermal and coordination aspects of transition metal complexes with uninegative bidentate Schiff base (HSB). The structure of the Schiff base is shown in Fig. 1.

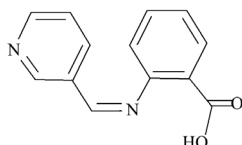


Fig. 1 Structure of the Schiff base (HSB)

Experimental

Materials

Reagent and solvents

All the chemicals used were of analytical grade. Metal nitrates and *o*-amino benzoic acid were purchased from E. Merck (India) Ltd., Mumbai. Pyridine-3-carboxyaldehyde was purchased from Fluka. The organic solvents were purified by standard methods [14].

Synthesis of pyridine-*m*-carboxaldene-*o*-aminobenzoic acid (HSB)

An ethanolic solution (100 mL) of pyridine-3-carboxyaldehyde (10 mmol, 1.07 g) and an ethanolic solution (100 mL) of *o*-aminobenzoic acid (10 mmol, 1.37 g) in 1:1 molar ratio were mixed with constant stirring. Refluxing was carried out for 5 h. The solution was cooled overnight at room temperature. The formed light brown crystals were collected and dried in air. Yield: 1.85 g (76%); *m.p.*: 232°C.

Synthesis of the metal complexes

The preparation of complexes was carried out by mixing methanolic solution (100 mL) of metal nitrate (10 mmol) and a hot DMF solution of the Schiff base (20 mmol, 4.52 g) in 1:2 molar ratio. The resulting

* Author for correspondence: jeenenpatel@yahoo.co.in

mixture was stirred under reflux for 4 h at 70°C. The obtained coloured crystals were collected by filtration, washed with water, methanol and finally with diethyl ether and dried in air.

Methods

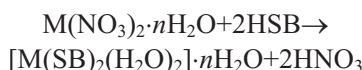
The metal content of the complexes were determined by the EDTA titration technique [15] after decomposing the organic matter with a mixture of HClO_4 , H_2SO_4 and HNO_3 (1:1.5:2.5). Carbon, hydrogen and nitrogen were analyzed with the Perkin Elmer, USA 2400-II CHN analyzer. The magnetic moments were obtained by the Gouy's method using mercury tetrathiocyanato cobaltate(II) as a calibrant ($\chi_g=16.44 \cdot 10^{-6}$ c.g.s. units at 20°C). Diamagnetic corrections were made using Pascal's constant.

A simultaneous TG/DTG and DTA had been obtained by a model 5000/2960 SDT, TA Instruments, USA. The experiments were performed in N_2 atmosphere at a heating rate of 10°C min⁻¹ in the temperature range 50–800°C, using Al_2O_3 crucible. The sample sizes are ranged in mass from 4.5–10 mg. DSC was recorded using DSC 2920, TA Instrument, USA. DSC curves were obtained at a heating rate of 10°C min⁻¹ in N_2 atmosphere over the temperature range of 50–400°C, using aluminium crucible. The IR spectra were recorded on a FTIR Nicolet 400D spectrophotometer using KBr pellets. The reflectance spectra of the complexes were recorded in the range of 1700–350 nm (as MgO discs) on a Beckman DK-2A spectrophotometer.

Results and discussion

The analytical and physical data of the ligand and its metal complexes are presented in Table 1. The com-

plexes are coloured and stable in air. They are insoluble in water, alcohol and DMF but least soluble in DMSO. The formations of the complexes are assumed according to the following balanced chemical equations:



where $\text{M}=\text{Mn}(\text{II}), \text{Co}(\text{II}), \text{Ni}(\text{II}), \text{Cu}(\text{II}), \text{Zn}(\text{II})$ and $\text{Cd}(\text{II})$.

Infrared spectra

IR spectra of the Schiff base (HSB) and its metal complexes were recorded as KBr disks and are summarized with some tentative assignments of important characteristic bands. The infrared spectral data of the metal complexes are shown in Table 2.

In the investigated complexes, the bands observed in the region 3200–3400, 1270–1310, 830–860 and 700–720 cm⁻¹ are attributed to OH stretching, bending, rocking and wagging vibrations, respectively due to the presence of water molecules [16]. In the spectra of the Schiff base, a strong band at 1669 cm⁻¹ is attributable to the –C=N group. On coordination, due to possible drift of the lone pair density towards the metal ion, the azomethine –C=N bond is expected to absorb at ~1622–1629 cm⁻¹ indicates the coordination of the azomethine nitrogen to the metal ion [17]. In all the metal chelates, a new band is seen in the 500–510 cm⁻¹ region, which is probably due to the formation of M–N bonds [18].

The concept of the thermal stability order of the metal complexes can be explained on the basis of the separation (Δ) between carboxylate anti-symmetric and symmetric stretching frequencies for the C–O bonds of the metal complexes. As the covalent character of the M–O bond increases, the anti-symmetric

Table 1 Analytical and physical data of the Schiff base (HSB) and its metal complexes^a

Compound	Colour	Found (calc.)/%				$\mu_{\text{eff}}/\text{B.M.}$	Yield/%
		C	H	N	M		
Ligand	light green	69.10 (69.02)	4.45 (4.42)	12.39 (12.38)	—	—	76
$[\text{Mn}(\text{SB})_2(\text{H}_2\text{O})_2] \cdot 2.5\text{H}_2\text{O}$	dark brown	53.26 (53.24)	4.56 (4.60)	9.58 (9.55)	9.39 (9.37)	5.97	66
$[\text{Co}(\text{SB})_2(\text{H}_2\text{O})_2] \cdot 2.5\text{H}_2\text{O}$	dark brown	52.96 (52.88)	4.59 (4.50)	9.50 (9.49)	10.03 (9.98)	4.02	66
$[\text{Ni}(\text{SB})_2(\text{H}_2\text{O})_2] \cdot 3\text{H}_2\text{O}$	yellowish green	52.14 (52.11)	4.71 (4.67)	9.37 (9.35)	9.86 (9.80)	2.86	74
$[\text{Cu}(\text{SB})_2(\text{H}_2\text{O})_2] \cdot 2.5\text{H}_2\text{O}$	dark brown	52.52 (52.47)	4.57 (4.54)	9.44 (9.41)	10.72 (10.68)	1.78	72
$[\text{Zn}(\text{SB})_2(\text{H}_2\text{O})_2] \cdot 2.5\text{H}_2\text{O}$	light yellow	52.32 (52.31)	4.58 (4.52)	9.35 (9.38)	10.98 (10.96)	diamag.	68
$[\text{Cd}(\text{SB})_2(\text{H}_2\text{O})_2] \cdot 3\text{H}_2\text{O}$	light yellow	47.83 (47.82)	4.33 (4.29)	8.64 (8.58)	17.26 (17.23)	diamag.	70

^aHSB=pyridine-*m*-carboxaldene-*o*-aminobenzoic acid (the same in Tables 2–5)

Table 2 The characteristic IR bands of the ligand and the complexes

Compound	ν_{OH}	$\nu_{\text{C}=\text{N}}$	$\nu_{\text{C}=\text{C}}$	ν_{COO}			$\nu_{\text{M}-\text{N}}$	$\nu_{\text{M}-\text{O}}$
				antisymmetric	symmetric	$\Delta\nu$		
Ligand	3440	1669	1550	1624.00	1384.00	240.00	—	—
[Mn(SB) ₂ (H ₂ O) ₂]·2.5H ₂ O	3420	1626	1578	1582.18	1379.30	202.88	500	485
[Co(SB) ₂ (H ₂ O) ₂]·2.5H ₂ O	3447	1622	1570	1596.25	1362.00	234.25	502	474
[Ni(SB) ₂ (H ₂ O) ₂]·3H ₂ O	3444	1628	1555	1595.50	1374.00	221.50	509	490
[Cu(SB) ₂ (H ₂ O) ₂]·2.5H ₂ O	3435	1625	1560	1592.10	1379.00	213.10	502	478
[Zn(SB) ₂ (H ₂ O) ₂]·2.5H ₂ O	3442	1629	1574	1590.20	1382.50	207.70	510	485
[Cd(SB) ₂ (H ₂ O) ₂]·3H ₂ O	3429	1628	1568	1585.54	1384.30	201.24	505	485

stretching frequency should also increase and the symmetric stretching frequency should decrease. More importantly the separation between the two frequencies increases (Table 2), the thermal stability of the metal complexes are also increases [19, 20]. Based on the separation (Δ) between stretching frequencies for the carboxylate in HSB, the thermal stability of the metal complexes in decreasing order is: Co>Ni>Cu>Zn>Mn>Cd.

Magnetic moments and electronic spectra

The electronic spectra of the Mn(II) complex shows absorption bands at ~ 15000 , ~ 20000 and $\sim 25000 \text{ cm}^{-1}$ assignable to ${}^6\text{A}_{1g} \rightarrow {}^4\text{T}_{1g}$, ${}^6\text{A}_{1g} \rightarrow {}^4\text{T}_{2g}$ and ${}^6\text{A}_{1g} \rightarrow {}^4\text{A}_{1g}$, ${}^4\text{E}_g$ transitions, respectively, in an octahedral environment around the Mn(II) ion [21]. The magnetic moment value of the Mn(II) complex is 5.99 B.M. due to a high-spin d^5 -system with an octahedral geometry [22]. The observed magnetic moments 4.02 and 2.86 B.M., for the Co(II) [23] and Ni(II) [24] complexes, respectively, are within the range for an octahedral geometry. The electronic spectra of the Co(II) complex exhibits three bands at ~ 9400 , ~ 18500 and $\sim 19000 \text{ cm}^{-1}$, which may reasonably be assigned to ${}^4\text{T}_{1g}(\text{F}) \rightarrow {}^4\text{T}_{2g}(\text{F})$, ${}^4\text{T}_{1g}(\text{F}) \rightarrow {}^4\text{A}_{2g}(\text{F})$ and ${}^4\text{T}_{1g}(\text{F}) \rightarrow {}^4\text{T}_{1g}(\text{P})$ transitions, respectively. The electronic spectra of the Ni(II) complex also shows three bands at ~ 10500 , ~ 17500 and $\sim 24600 \text{ cm}^{-1}$ assignable to ${}^3\text{A}_{2g}(\text{F}) \rightarrow {}^3\text{T}_{2g}(\text{F})$, ${}^3\text{A}_{2g}(\text{F}) \rightarrow {}^3\text{T}_{1g}(\text{F})$ and ${}^3\text{A}_{2g}(\text{F}) \rightarrow {}^3\text{T}_{1g}(\text{P})$ transitions, respectively. The observed magnetic moment value of the Cu(II) complex is 1.78 B.M. and the band observed

at $\sim 15200 \text{ cm}^{-1}$ (${}^2\text{E}_g \rightarrow {}^2\text{T}_{2g}$ transition) in the electronic spectra of Cu(II) complex [25] suggest an octahedral geometry. The Zn(II) and Cd(II) complexes are diamagnetic as expected for d^{10} systems. The values of the electronic parameters, such as the ligand field splitting energy (10 Dq), Racah interelectronic repulsion parameter (B), nephelauxetic ratio (β) and ratio ν_2/ν_1 are summarized in Table 3. The suggested structure of the complexes is shown in Fig. 2.

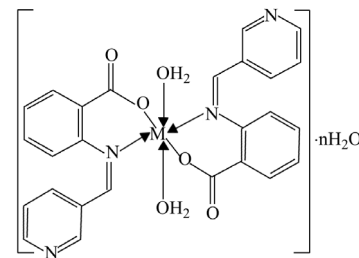
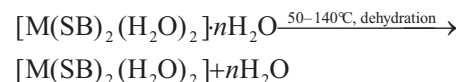


Fig. 2 Suggested structure of the metal complexes where $M=\text{Mn(II)}$, Co(II) , Cu(II) and Zn(II) , $n=2.5\text{H}_2\text{O}$; $M=\text{Ni(II)}$ and Cd(II) , $n=3\text{H}_2\text{O}$

Thermal studies

In general, the stages of thermal decomposition of the complexes can be written as shown:



where $M=\text{Mn(II)}$, Co(II) , Cu(II) and Zn(II) ($n=2.5$), $M=\text{Ni(II)}$ and Cd(II) ($n=3$).

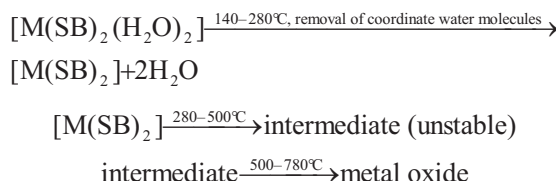
Table 3 Electronic parameters of the Co(II) and Ni(II) complexes^a

Complex	Observed bands/cm ⁻¹			ν_2/ν_1	B	β	β_0	10 Dq
	ν_1	ν_2	ν_3					
[Co(SB) ₂ (H ₂ O) ₂]·2.5H ₂ O	9400	18500	19000	1.97	715	0.73	26.4	10521
[Ni(SB) ₂ (H ₂ O) ₂]·3H ₂ O	10500	17500	24600	1.66	707	0.69	31.4	10500

^aThe ligand field splitting energy (10 Dq), interelectronic repulsion parameter (B) and covalency factor (nephelauxetic ratio) (β) for the Co(II) and Ni(II) complexes were calculated using the secular equations given by König [26]:

$$\begin{aligned} \text{For Co(II) complex} & \quad \text{For Ni(II) complex} \\ 10 \text{ Dq} &= 1/2[(2\nu_1 - \nu_3) + (\nu_3^2 + \nu_1\nu_3 - \nu_1^2)^{1/2}] & 10 \text{ Dq} &= \nu_1 \\ 15B &= \nu_3 - 2\nu_1 + 10 \text{ Dq} & 15B &= (\nu_2 + \nu_3) - 3\nu_1 \\ \beta = B/B_0 & [B_0 \text{ (free ion)} = 971] & \beta = B/B_0 & [B_0 \text{ (free ion)} = 1030] \\ \beta_0 &= (1-\beta) \cdot 100 & \beta_0 &= (1-\beta) \cdot 100 \end{aligned}$$

For the anhydrous complexes:



The anhydrous Schiff base complexes show great thermal stability up to 250°C; and in the third and subsequent stages, the decomposition and combustion of ligand (HSB) in the complexes occur. The nature of the intermediates formed in the third and later stages are not known, but they undergo violet decomposition to give the respective metal oxides as the final product.

Calculation of activation thermodynamic parameters of the decomposed complexes

The thermodynamic activation parameters of the decomposition process of the complexes such as energy of activation (E_a) and order of reaction (n) were evaluated graphically by employing the Freeman–Carroll [27] method using the following relation:

$$\begin{aligned} [(-E_a/2.303R)\Delta(1/T)]/\Delta\log w_r &= \\ &= -n + \Delta\log(dw/dt)/\Delta\log w_r \end{aligned} \quad (1)$$

where T is the temperature in K, R is gas constant, $w_r = w_c - w$; w_c is the mass loss at the completion of the reaction and w is the total mass loss up to time t . E_a and n are the energy of activation and order of reaction, respectively. A typical curve of $[\Delta\log(dw/dt)/\Delta\log w_r]$ vs. $[\Delta(1/T)/\Delta\log w_r]$ for the Zn(II) complex is shown in Fig. 3. The slope of the plot gave the value of $E_a/2.303R$ and the order of reaction (n) was determined from the intercept.

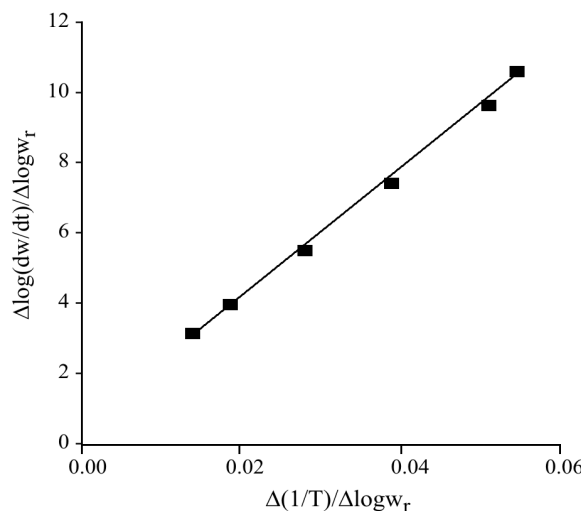


Fig. 3 Freeman–Carroll plot for thermal dehydration of $[\text{Zn}(\text{SB})_2(\text{H}_2\text{O})_2] \cdot 2.5\text{H}_2\text{O}$

The thermodynamic activation parameters of the decomposition process of dehydrated complexes such as entropy (S^*), preexponential factor (A), enthalpy (H^*) and free energy of the decomposition (G^*), were calculated using the following relations [28, 29]:

$$E_a/RT_s^2 = A/\Phi \exp(-E_a/RT_s) \quad (2)$$

$$S^* = 2.303(\log Ah/KT)R \quad (3)$$

$$H^* = E_a - RT \quad (4)$$

$$G^* = H^* - T_s S^* \quad (5)$$

where Φ is the heating rate, K is the Boltzman constant, h is the Plank constant and T_s is the peak temperature from DTG curve. According to the kinetic data obtained from DTG curves, all the complexes have negative entropy, which indicates that the studied complexes have more ordered systems than reactants [30].

The thermal behavior of the prepared complexes

In the following paragraphs the thermal behaviour of the synthesized complexes, characterized on the basis of TG/DTG, DTA and DSC methods are described. Thermal data and kinetic parameters of the complexes are given in Tables 4 and 5, respectively.

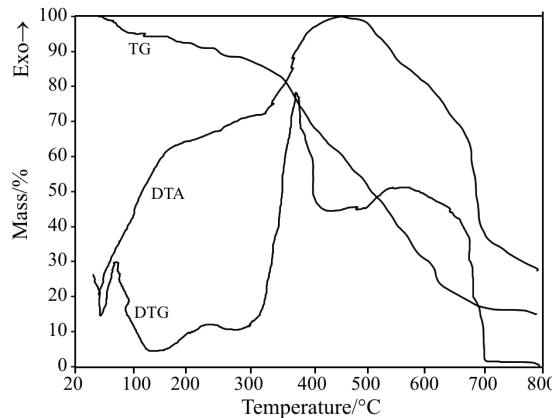
$[\text{Zn}(\text{SB})_2(\text{H}_2\text{O})_2] \cdot 2.5\text{H}_2\text{O}$

TG/DTG, DTA and DSC curves of the complex $[\text{Zn}(\text{SB})_2(\text{H}_2\text{O})_2] \cdot 2.5\text{H}_2\text{O}$ are represented in Figs 4 and 5, respectively. The $[\text{Zn}(\text{SB})_2(\text{H}_2\text{O})_2] \cdot 2.5\text{H}_2\text{O}$ complex undergoes decomposition in four stages. The first DTG peak at 69°C, in the temperature range 50–140°C, with the mass loss (obs. 7.57%; calc. 7.54%) corresponds to the loss of two and half moles of lattice water molecules. DTA curve shows an endothermic peak at 76°C. This process is further supported by an endothermic peak [31] at 128°C in DSC curve. The loss of two and half moles of lattice water molecules is a first order and the value of the energy of activation for the dehydration process is found to be $3.851 \text{ kJ mol}^{-1}$. The second stage between 140 and 280°C corresponds to the decomposition of two coordinated water molecules [32]. The observed mass loss is 5.96% which is consistent with the theoretical value of 6.03%. This process is accompanied by an endothermic peak at 226.47°C in DSC curve [33]. With heating; the decomposition of the ligand moiety was followed. Two well-separated peaks are displayed on the DTG curve; this indicates that the decomposition of the ligand (HSB) divides into two steps. The third stage, which occurs in the temperature range 280–400°C, with a DTG peak at 379°C, corresponds to the decomposition of one part of the ligand. The observed mass loss for this stage is 17.38%. It is further supported by

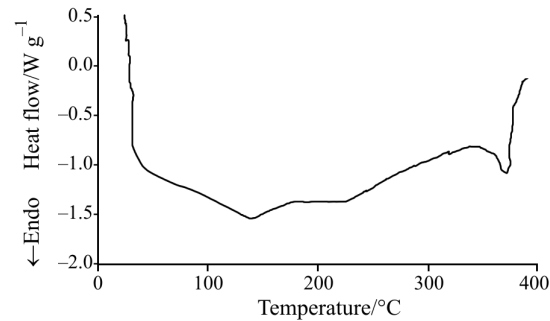
Table 4 Thermoanalytical results (TG, DTG and DTA) of the divalent metal complexes of HSB

Complex	TG range/ °C	DTG _{max} / °C	DTA _{max} / °C	Mass loss/% obs. (calc.)	Assignment
[Mn(SB) ₂ (H ₂ O) ₂]·2.5H ₂ O	50–130	68	75(+)	7.58 (7.67)	loss of 2.5 lattice water molecules
	130–250	189	—	6.26 (6.14)	loss of 2 coordinated water molecules
	250–470	420	393(—)	38.52	removal of one part of the ligand
	470–650	573	570(—)	35.40 87.76* (87.87)	removal of remaining part of the ligand leaving MnO residue
[Co(SB) ₂ (H ₂ O) ₂]·2.5H ₂ O	50–190	79	82(+)	13.89 (13.73)	loss of 4.5 water molecules
	190–490	313	—	17.67	removal of one part of the ligand
	490–780	526	521(—)	40.28 71.75* (71.87)	removal of remaining part of the ligand leaving Co ₂ O ₃ residue
[Ni(SB) ₂ (H ₂ O) ₂]·3H ₂ O	50–130	74	81(+)	9.28 (9.01)	loss of 3 lattice water molecules
	130–240	198	—	5.97 (6.01)	loss of 2 coordinated water molecules
	240–390	282	294(—)	18.1	removal of one part of the ligand
	390–490	438	—	19.48	removal of second part of the ligand
	490–650	535	527(—)	34.92 87.65* (87.44)	removal of remaining part of the ligand leaving NiO residue
[Cu(SB) ₂ (H ₂ O) ₂]·2.5H ₂ O	50–130	70	78(+)	7.61 (7.56)	loss of 2.5 lattice water molecules
	130–230	186	—	5.98 (6.05)	loss of 2 coordinated water molecules
	230–370	268	281(—)	17.31	removal of one part of the ligand
	370–780	462	—	55.66 86.56* (86.60)	removal of remaining part of the ligand leaving CuO residue
[Zn(SB) ₂ (H ₂ O) ₂]·2.5H ₂ O	50–140	69	76(+)	7.57 (7.54)	loss of 2.5 lattice water molecules
	140–280	216	—	5.96 (6.03)	loss of 2 coordinated water molecules
	280–400	379	390(—)	17.38	removal of one part of the ligand
	400–780	668	679(—)	55.61 86.31* (86.34)	removal of remaining part of the ligand leaving ZnO residue
[Cd(SB) ₂ (H ₂ O) ₂]·3H ₂ O	50–130	67	72(+)	8.22 (8.27)	loss of 3 lattice water molecules
	130–250	194	—	5.34 (5.51)	loss of 2 coordinated water molecules
	250–520	361	366(—)	34.15	removal of one fragment of the ligand
	520–650	568	555(—)	32.37 80.18* (80.30)	removal of remaining part of the ligand leaving CdO residue

(+) – endothermic; (—) – exothermic; *total mass loss

**Fig. 4** TG, DTG and DTA curves of [Zn(SB)₂(H₂O)₂]·2.5H₂O

an endothermic peak at 373°C in DSC curve. The fourth stage occurs between 400 and 780°C, corresponding to the decomposition of the remaining part of the ligand, with the mass loss of 55.61%. The maximum rate of mass loss is indicated by the DTG peak at 550°C. The total mass loss (86.31%) coincides with the theoretical value of 86.34% (Table 4). The final residue, estimated as zinc oxide.

**Fig. 5** DSC curve of [Zn(SB)₂(H₂O)₂]·2.5H₂O[Mn(SB)₂(H₂O)₂]·2.5H₂O

The thermal decomposition of the complex [Mn(SB)₂(H₂O)₂]·2.5H₂O undergoes in four stages. The thermal dehydration begins at 50°C and ends at 130°C with a DTG peak at 68°C. The observed mass loss (7.58%) is attributed to the decomposition of two and half moles of lattice water molecules (theoretical mass loss: 7.67%). The DTA curve shows an endothermic peak at 75°C. The thermal dehydration is of first order and the energy of activation is found to

Table 5 Thermodynamic data of the thermal decomposition of metal complexes

Complex	TG range/°C	$E_a/\text{kJ mol}^{-1}$	n	A/s^{-1}	$S^*/\text{J K}^{-1} \text{mol}^{-1}$	$H^*/\text{kJ mol}^{-1}$	$G^*/\text{kJ mol}^{-1}$
[Mn(SB) ₂ (H ₂ O) ₂]·2.5H ₂ O	50–130	3.81	0.96	0.010	-284	0.974	97.9
	130–250	4.79	1.48	0.093	-268	0.949	125
	250–470	8.85	1.00	0.103	-271	3.092	191
	470–630	79.09	1.00	1.01·10 ⁴	-177	72.06	222
[Co(SB) ₂ (H ₂ O) ₂]·2.5H ₂ O	50–190	4.89	0.98	0.008	-286	1.969	102
	190–490	9.34	1.20	0.223	-263	4.477	159
	490–780	100.8	1.00	0.73·10 ⁶	-141	94.13	207
[Ni(SB) ₂ (H ₂ O) ₂]·3H ₂ O	50–120	4.59	0.96	0.009	-285	1.70	101
	120–240	4.83	1.49	0.090	-269	0.922	128
	240–380	10.81	1.10	0.438	-257	6.196	149
	380–480	24.38	1.01	0.35·10 ¹	-242	18.46	190
[Cu(SB) ₂ (H ₂ O) ₂]·2.5H ₂ O	50–130	3.90	0.97	0.010	-284	1.052	98.5
	130–230	5.12	1.39	0.112	-267	1.308	124
	230–370	10.55	1.00	0.452	-257	6.052	145
	370–780	55.81	1.00	1.02·10 ³	-195	49.07	192
[Zn(SB) ₂ (H ₂ O) ₂]·2.5H ₂ O	50–130	3.85	0.98	0.010	-284	1.006	98.2
	130–280	4.92	1.51	0.083	-270	0.857	133
	280–400	13.06	1.00	0.412	-259	7.646	176
	400–780	59.74	1.00	1.66·10 ²	-212	51.91	252
[Cd(SB) ₂ (H ₂ O) ₂]·3H ₂ O	50–130	3.77	0.97	0.010	-284	0.948	97.6
	130–210	4.81	1.49	0.091	-269	0.929	126
	210–510	8.10	1.10	0.112	-269	2.829	174
	510–650	88.41	1.00	1.95·10 ⁴	-172	80.98	235

be 3.810 kJ mol⁻¹. The second stage is related to the liberation of two coordinated water molecules from the complex in the temperature range of 130–250°C, accompanied by a mass loss of 6.26% (calc. 6.14%). The maximum rate of mass loss is indicated by the DTG peak at 189°C. The third stage, which occurs in the temperature range 250–470°C with a DTG peak at 420°C, corresponding to the decomposition of one part of the ligand. The observed mass loss for this stage is 38.52%. This process is further supported by an exothermic peak at 393°C in DTA curve. The fourth stage is related to the decomposition of the remaining part of the ligand in the temperature range of 470–650°C with a DTG peak at 573°C, accompanied by a mass loss of 35.40%. The overall mass losses are observed to be 87.76%, which is in well agreement with the calculated value of 87.87%. The final residue, estimated as manganese oxide, has the observed mass 12.23% as against the calculated value of 12.10%.

[Co(SB)₂(H₂O)₂]·2.5H₂O

The thermal decomposition of the complex [Co(SB)₂(H₂O)₂]·2.5H₂O undergoes in three stages. The thermal dehydration of this complex takes place in a single step between 50 and 190°C, with a mass loss of 13.8% (calc. 13.73%). The maximum rate of mass loss is indicated by the DTG peak at 79°C. Two and half moles of lattice water molecules and two moles of coordinated water molecules are removed in this stage of dehydration. This process is accompa-

nied by endothermic effects at 82 and 159°C in DTA and DSC curves, respectively. The total loss of two and half moles of lattice water molecules and two moles of coordinated water molecules is a first order reaction and the value of the energy of activation for the dehydration process is 4.896 kJ mol⁻¹. With heating, the decomposition of the ligand was followed. Two well-separated peaks are displayed on the DTG curve; this indicates that the decomposition of the ligand divides into two steps. The temperature range 190–490°C with a DTG peak at 313°C, corresponding to the decomposition of one part of the ligand. The observed mass loss for this stage is 17.67%. The endothermic peak at 318°C corresponds to this stage is given by DSC curve. The third stage, which occurs in the temperature range 490–780°C, corresponds to the decomposition of the remaining part of the ligand. The observed mass loss for this stage is 40.28%. The overall mass loss 71.75% is as against the theoretical value (71.87%). The end product estimated as Co₂O₃, has the observed mass of 28.25% compared with the calculated value of 28.11%.

[Ni(SB)₂(H₂O)₂]·3H₂O

The thermal decomposition of the complex [Ni(SB)₂(H₂O)₂]·3H₂O undergoes in five stages. The first DTG peak at 74°C, in the temperature range 50–130°C, with the mass loss (obs. 9.28%; calc. 9.01%) corresponds to the loss of three lattice water molecules [34, 35]. This process is further supported by en-

dothermic effects at 81 and 116°C in DTA and DSC curve, respectively. The loss of three lattice water molecules is a first order and the value of the energy of activation for the dehydration process is 4.594 kJ mol⁻¹. The second stage occurs in the temperature range 130–240°C, with the mass loss (5.97%) is due to the removal of two coordinated water molecules from the complex (calc. 6.01%). The DTG peak corresponding to this stage is found at 198°C. This process is further supported by an endothermic peak at 190°C in DSC curve. With heating, the decomposition of ligand was followed. The third (from 240–390°C), fourth (from 390–490°C) and fifth (from 490–650°C) stages may be due to the decomposition of the ligand molecule. The observed mass losses for these temperature ranges are 18.1, 19.48 and 34.82%, respectively. The overall mass losses are observed to be 87.65%, which is in well agreement with the calculated value of 87.44%. The final residue, estimated as nickel oxide, has the observed mass 12.32% as against the calculated value of 12.47%.

[Cu(SB)₂(H₂O)₂]·2.5H₂O

The thermal decomposition of the complex [Cu(SB)₂(H₂O)₂]·2.5H₂O takes place in four distinct stages. The first stage starts at 50 and ends at 130°C, with a DTG peak at 70°C. The observed mass loss (7.61%) is attributed to the decomposition of two and half moles of crystallized water molecules (calc. 7.56%). This process is further supported by an endothermic peak at 78°C in DTA curve. The activation energy for this dehydration step is equal to 3.902 kJ mol⁻¹ and the order of reaction for the dehydration process is found to be one. The second stage is related to the decomposition of two coordinated water molecules from the complex in the temperature range 130–230°C with a DTG peak at 186°C. The observed mass loss is 5.98%, which is consistent with the theoretical value of 6.05%. The broad endothermic peak at 123°C corresponding to the removal of water molecules from the complex is given by DSC curve. The third stage, which occurs in the temperature range 230–350°C with a DTG peak at 268°C, corresponding to the decomposition of one part of the ligand. The observed mass loss is 17.31%. The DSC peak corresponding to this stage is 279°C. The fourth stage is related to the decomposition of remaining part of the ligand, in the temperature range of 350–780°C with the DTG peak at 462°C, accompanied by a mass loss of 55.66%. The total mass loss (86.56%) is coincides with the theoretical value of 86.60%. The end product estimated as copper oxide.

[Cd(SB)₂(H₂O)₂]·3H₂O

The complex [Cd(SB)₂(H₂O)₂]·3H₂O undergoes thermal decomposition in four stages. The thermal dehydration of this complex takes place between 50 and 130°C, with a mass loss of 8.22% (calc. 8.27%). The maximum rate of mass loss is indicated by the DTG peak at 67°C. Three moles of lattice water molecules are removed in this stage of dehydration. This process is accompanied by endothermic effects at 72 and 122°C in DTA and DSC curve, respectively. The loss of three lattice water molecules is a first order reaction and the value of the energy of activation for the dehydration process is 3.777 kJ mol⁻¹. This is followed immediately by the second mass loss (obs. 5.3%; calc. 5.5%) within the temperature range 130–250°C with a DTG peak at 194°C, corresponds to the liberation of two coordinated water molecules. This process is accompanied by an endothermic peak at 228°C in DSC curve. The third (from 250–520°C) and the fourth (from 520–650°C) stages may be due to the pyrolysis of ligand moiety. The observed mass losses for these temperature ranges are 34.15 and 32.37%, respectively. The overall mass losses are observed to be 80.18%, which is in well agreement with the calculated value of 80.30%, and the final residue estimated as CdO.

In order to discuss the thermal stability in the solid-state, a plot of the reciprocal ionic radii of the divalent metal ions against the atomic number exhibits some definite trends as shown in Fig. 6. The metal ions follow the sequence: Ni(II)>Cu(II)>Zn(II)>Co(II)>Mn(II)>Cd(II).

The initial temperatures of decomposition (dehydration) of the complexes were taken for comparative purposes. A plot of the initial decomposition temperatures of the complexes against the atomic number exhibits some definite trends as shown in Fig. 7. The thermal stabilities of the complexes follow the sequence: Co(II)>Ni(II)>Cu(II)>Zn(II)>Mn(II)>Cd(II).

These orders are in good agreement with the order predicted from the IR spectra, on the basis of separa-

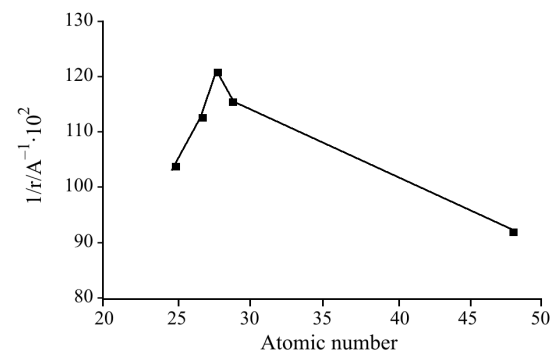


Fig. 6 Reciprocals of ionic radii of divalent metal ions vs. atomic number

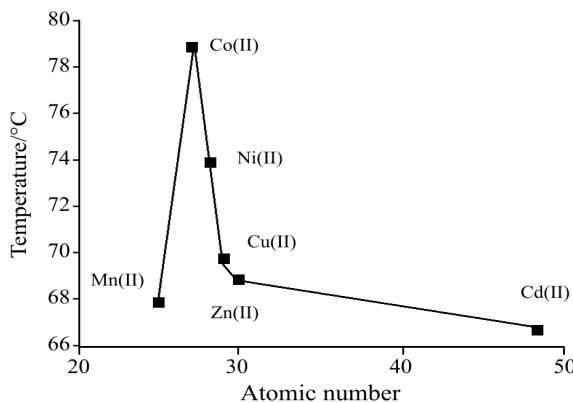


Fig. 7 Initial tempeatures of decomposition of the complexes vs. atomic number

tion (Δ) between stretching frequencies for the carboxylate ion in HSB. It is evident that the thermal stabilities of the complexes increase as the ionic radii decrease. The thermal stabilities of the Ni(II), Cu(II), Zn(II), Mn(II) and Cd(II) complexes in the solid-state follow the general trend found by Irving and Williams [36] for the stabilities of complexes in solution. The Co(II) complex deviate from this general behaviour. Since the Irving–Williams series reflects electrostatic effects, this observation indicates that the water–metal interaction in these complexes is almost of ion-dipole type. A similar relationship was observed in the case of the double ammonium sulfate hexahydrate salts of the first raw transition metals [37].

Acknowledgements

We wish to express our gratitude to the Head, Department of Chemistry, Sardar Patel University, Vallabh Vidyanagar, India, for providing the necessary laboratory facilities.

References

- G. G. Mohamed and Z. H. Abd El-Wahab, *J. Therm. Anal. Cal.*, 73 (2003) 347.
- P. A. Vigato and S. Tamburini, *Coord. Chem. Rev.*, 248 (2004) 717.
- R. Hernandez-Molina and A. Mederos, In *Comprehensive Coordination Chemistry-II*, Vol. 1, Elsevier-Pergamon Press, Oxford–New York 2003, p. 411.
- M. Arshad, Saeed-ur-Rehman, S. Ali Khan, K. Masud, N. Arshad and A. Ghani, *Thermochim. Acta*, 364 (2002) 143.
- N. Deb, S. D. Baruah, N. Sen Sarma and N. N. Dass, *Thermochim. Acta*, 320 (1998) 53.
- A. A. Soliman, *J. Therm. Anal. Cal.*, 63 (2001) 221.
- A. F. Petrovic, D. M. Petrovic, V. M. Zeovac and M. Budimir, *J. Therm. Anal. Cal.*, 58 (1999) 589.
- M. A. Zayed and F. A. Nour El-Dien, *Thermochim. Acta*, 114 (1987) 359.
- G. G. Mohamed, F. F. Nour-El Dien and E. A. El-Gamed, *J. Therm. Anal. Cal.*, 67 (2002) 135.
- R. Kucsera, D. Joniakarà and L. Žuková, *J. Therm. Anal. Cal.*, 78 (2004) 263.
- S. Gao, S. Chen, G. Xie, G. Fan and Q. Shi, *J. Therm. Anal. Cal.*, 81 (2005) 387.
- H. M. Parekh, P. K. Panchal and M. N. Patel, *J. Therm. Anal. Cal.*, OnlineFirst, DOI: 10.1007/s10973-005-7284-5.
- H. M. Parekh and M. N. Patel, *Russ. J. Coord. Chem.*, 32 (2006) 431.
- A. I. Vogel, *Textbook of Practical Organic Chemistry*, 5th Edn. Longman, London 1989.
- A. I. Vogel, *A Textbook of Quantitative Inorganic Analysis*, Longmans Green, London 1962.
- N. Nakamoto, *Infrared spectra and Raman spectra of inorganic and coordination compounds*, John Wiley & Sons, New York 1978.
- R. K. Agarwal, H. Agarwal and I. Chakraborti, *Synth. React. Inorg. Met.-Org. Chem.*, 25 (1999) 679.
- E. M. Jouad, A. Riou, M. Allain, M. A. Khan and G. M. Bouet, *Polyhedron*, 20 (2001) 67.
- R. S. Bottel, H. Chang and D. A. Lusardi, *J. Inorg. Nucl. Chem.*, 41 (1979) 909.
- T. Premkumar and S. Govindarajan, *J. Therm. Anal. Cal.*, 84 (2006) 395.
- N. H. Patel, H. M. Parekh and M. N. Patel, *Trans. Met. Chem.*, 30 (2005) 13.
- H. M. Parekh, S. R. Mehta and M. N. Patel, *Russ. J. Inorg. Chem.*, 51 (2006) 67.
- P. K. Panchal and M. N. Patel, *Synth. React. Inorg. Met.-Org. Chem.*, 34 (2004) 1277.
- R. K. Agarwal, P. Garg, H. Agarwal and S. Chandra, *Synth. React. Inorg. Met.-Org. Chem.*, 27 (1997) 251.
- H. Koksal, M. Dolaz, M. Tilmer and S. Serin, *Synth. React. Inorg. Met.-Org. Chem.*, 31 (2001) 1141.
- E. König, *The nephelauxetic effect. In Structure and Bonding*, Springer Verlag, New York 1971, pp. 9, 175.
- E. S. Freeman and B. Carroll, *J. Phys. Chem.*, 62 (1958) 394.
- M. Nath and P. Arora, *Synth. React. Met.-Org. Chem.*, 23 (1993) 1523.
- M. Sekerci and F. Yakuphanoglu, *J. Therm. Anal. Cal.*, 75 (2004) 189.
- G. G. Mohamed, F. A. Nour El-Dien and N. E. A. El-Gamel, *J. Therm. Anal. Cal.*, 67 (2002) 135.
- J. E. House Jr. and J. C. Bailar Jr., *J. Inorg. Nucl. Chem.*, 38 (1976) 1791.
- H. A. El-Boraey, *J. Therm. Anal. Cal.*, 81 (2005) 339.
- J. E. House Jr. and B. J. Smith, *J. Inorg. Nucl. Chem.*, 39 (1977) 777.
- M. Badea, R. Olar, D. Marinescu, G. Vasile and S. Stoleriu, *J. Therm. Anal. Cal.*, 80 (2005) 679.
- T. Premkumar, S. Govindarajan, W. P. Pan and R. Xie, *J. Therm. Anal. Cal.*, 74 (2003) 325.
- H. Irving and R. J. P. Williams, *J. Chem. Soc.*, (1953) 3192.
- V. T. Yilmaz, H. İçbudak and H. Ölmez, *Thermochim. Acta*, 244 (1994) 85.

Received: May 8, 2006

Accepted: September 5, 2006

OnlineFirst: December 18, 2006

DOI: 10.1007/s10973-006-7682-3